



Highly sensitive and selective determination of copper(II) based on a dual catalytic effect and by using silicon nanoparticles as a fluorescent probe

Xiaogen Chen¹ · Qiujuan Lu¹ · Dan Liu¹ · Cuiyan Wu¹ · Meiling Liu¹ · Haitao Li¹ · Youyu Zhang¹ · Shouzhao Yao¹

Received: 17 January 2018 / Accepted: 31 January 2018 / Published online: 19 February 2018
© Springer-Verlag GmbH Austria, part of Springer Nature 2018

Abstract

The authors describe a silicon nanoparticle-based fluorometric method for sensitive and selective detection of Cu^{2+} . It is based on the catalytic action of Cu^{2+} on the oxidation of cysteine (Cys) by oxygen to form cystine and the by-product H_2O_2 . The generated H_2O_2 is catalytically decomposed by Cu^{2+} to generate hydroxyl radicals which oxidize and destroy the surface of SiNPs. As a result, the blue fluorescence of the SiNPs is quenched. The method has excellent selectivity due to the dual catalytic effects of Cu^{2+} , which is much better than most previously reported nanomaterial-based assays for Cu^{2+} . Under the optimal conditions, the method has low detection limit (29 nM) and a linear response in a concentration range from 0.05 μM to 15 μM . The method has been successfully applied to the determination of Cu^{2+} in spiked real water samples, and the results agreed well with those obtained by the Chinese National Standard method (GB/T 7475-1987; AAS).

Keywords Copper ions · Cysteine · Cystine · Dual catalytic effects · Hydroxyl radicals · Fluorometry · Stern-Volmer plot · Quenching

Introduction

Copper is widely used in agriculture and industry, and also plays an important role in the environment and in human physiology. High concentrations of Cu^{2+} may be toxic to the

human body [1, 2] and lead to liver or kidney diseases [3]. For this reason, Cu^{2+} is listed as a priority pollutant by the Environmental Protection Agency (EPA) [4]. Therefore, the detection of the concentration of Cu^{2+} in environmental water samples has important practical value in the water pollution monitoring and management. Many analytical methods have been developed and utilized to detect Cu^{2+} including electrochemical method [5], atomic emission spectrometry [6], atomic absorption spectrometry [7], colorimetry [8–11], fluorometry [12] and so on. Among these methods, fluorometry has been proved to be an ideal technique for the trace analysis due to its advantages of easy operation and high sensitivity.

Various fluorometric methods for the detection of Cu^{2+} have been designed by utilizing fluorescence dyes or fluorescence nanomaterials as fluorescent probes [13–15]. However, many of them still suffer from some drawbacks, such as complicated synthetic procedures, poor water solubility and toxicity, which limit their further applications [16, 17]. On the other hand, most methods are based on the interaction between Cu^{2+} and the functional groups of fluorescence probes. However, some metal ions may influence the selectivity due to their similar chemical properties and ionic radii. For instance, utilizing the affinity effect between the amino group at the

Xiaogen Chen and Qiujuan Lu contributed equally to this work.

Research Highlights

- A fluorescence detection method for Cu^{2+} was developed based on the dual catalytic effects of Cu^{2+}
- Metal ions with similar chemical properties and ionic radius do not influence the selectivity
- The dual catalytic effect of Cu^{2+} improves selectivity

Electronic supplementary material The online version of this article (<https://doi.org/10.1007/s00604-018-2720-y>) contains supplementary material, which is available to authorized users.

✉ Youyu Zhang
zhangyy@hunnu.edu.cn

¹ Key Laboratory of Chemical Biology and Traditional Chinese Medicine Research (Ministry of Education), College of Chemistry and Chemical Engineering, Hunan Normal University, Changsha 410081, People's Republic of China

surface of carbon quantum dots and the Cu^{2+} , Chi et al. developed a fluorescence method to detect Cu^{2+} [18]. However, some cations, such as Ni^{2+} , Fe^{2+} and Hg^{2+} , seriously disturb the detection of Cu^{2+} due to the combinations of Ni^{2+} , Fe^{2+} and Hg^{2+} with amino groups. Based on the chelation of Cu^{2+} and the “N” and “O” atoms, Sun et al. developed a polymer nanodots-based fluorescence method to detect Cu^{2+} . Although satisfactory results were obtained, the selectivity results indicated that Fe^{3+} influence the selectivity [19]. Furthermore, similar phenomena are also found in some of the reported literatures [4, 19–21]. Therefore, smart design should be introduced for the construction of Cu^{2+} detection method with better selectivity.

It has been demonstrated that Cu^{2+} can not only catalyze the cysteine (Cys) to cystine and produce H_2O_2 under the O_2 atmosphere [22, 23], but also catalyze decomposition of as-produced H_2O_2 into hydroxyl radicals through Fenton-like reaction [24, 25]. In the present work, using silicon nanoparticles (SiNPs) which with low cytotoxicity, high biocompatibility, good hydrophilicity and stable fluorescence as fluorophore [26], the authors developed a novel method to detect Cu^{2+} based on the strong oxidizing properties of hydroxyl radicals which were produced by the dual catalytical effects of Cu^{2+} . The fluorescence of SiNPs was quenched significantly by hydroxyl radicals for oxidizing and destroying the surface state of SiNPs, which was proportional to the concentration of Cu^{2+} . This novel method shows high selectivity and sensitivity toward Cu^{2+} due to the unique dual catalytical effects of Cu^{2+} . Furthermore, the application of this method to detect Cu^{2+} in real water samples is also demonstrated successfully.

Experimental section

Reagents

(3-Aminopropyl)trimethoxysilane (APTMS) (97%) was purchased from Shanghai Energy Chemical Co., Ltd. (<http://www.energy-chemical.com/>). Other reagents were purchased from Sinopharm Chemical Reagent Co., Ltd. (<http://www.reagent.com.cn:666/ScrcBackGroup/reagent/newindex.jsp>), and used directly without further purification. HEPES (10 mM) buffer was prepared by dissolving 4-(2-hydroxyethyl)-1-piperazineethanesulfonic acid in ultrapure water and adjusting the pH value to 8.0 with 1 M NaOH. The ultrapure water from a Millipore system (resistance $\geq 18.2 \text{ M}\Omega \text{ cm}$) was used throughout the experiments.

Apparatus

The UV-vis absorption spectra were measured on a UV2450 spectrophotometer (Shimadzu CO., LTD, Japan). The fluorescence (FL) emission spectra were collected on an F-7000

spectrophotometer (Hitachi CO., LTD, Japan). The Fourier transform infrared (FT-IR) spectra were performed from Nicolet Nexus 670 FT-IR spectrometer (Nicolet Instrument CO., U.S.A.). The microstructures of the SiNPs were examined using a JEOL-1230 transmission electron microscope (JEOL CO., LTD, Japan).

Preparation of silicon nanoparticles and detection of Cu^{2+}

SiNPs were prepared according to the literature [26] (The detailed synthesis process was presented in [supplementary material](#)). The detection of Cu^{2+} was performed at environment temperature (about 20 °C) in pH 8.0, 10 mM HEPES buffer. Firstly, 20 μL SiNPs (600 $\mu\text{g mL}^{-1}$) solution and 10 μL Cys (50 mM) solution were mixed with 960 μL HEPES buffer. Then, 10 μL of varied concentrations of Cu^{2+} were added into the mixed solution. The above solutions were incubated for 30 min at environment temperature (about 20 °C). After that, the fluorescence emission spectra were recorded immediately under excitation wavelength at 350 nm. For comparison, other ions including Na^+ , K^+ , Ag^+ , Mg^{2+} , Ni^{2+} , Zn^{2+} , Ca^{2+} , Co^{2+} , Cd^{2+} , Hg^{2+} , Pb^{2+} , Mn^{2+} , Fe^{2+} , Fe^{3+} and Al^{3+} were also tested by the same conditions. Each experiment was repeated three times. The error bars represent standard deviation from 3 replicates.

Real water samples analysis

The tap water sample was collected from the lab's tap in the authors' institute. The mineral water was collected from the Yuelu mountain (Changsha, China). The river water was collected from the Xiangjiang river (Changsha, China). The real water samples (tap water, mineral water and river water) were simply filtered with cylinder membrane filter (0.22 μm , Pall 66,191, Pall Corporation, USA) and diluted 10 times before the analysis. The following steps were similar to that of fluorescence detection of Cu^{2+} , and the test solutions were spiked with standard solutions including varied concentration of Cu^{2+} . Besides, the analytical results were found by atomic absorption spectrometry (data were performed by an atomic absorption spectrophotometer, Beijing Purkinje General Instrument CO. LTD, China) and from the Chinese National Standard GB/T 7475-1987 (water quality—determination of copper, zinc, lead and cadmium—atomic absorption spectrometry).

Results and discussion

Choice of materials

The morphology and property of nanomaterials have important influence on the performance of fluorescence detection methods. Compared with semiconductor quantum dots (e.g.

CdSe, CdS and ZnS etc.), which are usually composed of heavy metals, SiNPs have the advantages of good water dispersibility, low toxicity, resistance to photobleaching and good biocompatibility [27]. On the other hand, the larger specific surface area and abundant surface functional groups of SiNPs make it easy interaction with guest species. Moreover, the SiNPs also have strong fluorescence, which is helpful to improve the detection sensitivity. Therefore, based on the above advantages, the authors developed a fluorescence method to detect Cu^{2+} by using SiNPs as fluorophore.

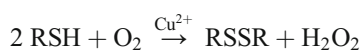
Characterization of SiNPs

Transition electron microscopy (TEM) experiments were performed to investigate the morphology of the SiNPs. Fig. 1a shows that a great deal of spherical nanoparticles can be observed in the TEM image and that the SiNPs possess excellent monodispersity and uniform size. The diameters were calculated to be about 6–8 nm (Fig. 1b). In order to demonstrate the surface structure of the SiNPs, the FT-IR spectra information was collected. As shown in Fig. 1c, the absorption peaks at 1100 cm^{-1} , 1384 cm^{-1} , 1577 cm^{-1} , and 3423 cm^{-1} are assigned to the Si-O stretching vibration C-O bending vibrations, N-H bending vibrations and the N-H stretching vibration, respectively. The FT-IR results indicated that amino groups are rich on the surface of SiNPs, which is similar with the literature [26]. In addition, as shown in Fig. 1d, the absorption, excitation and emission spectra demonstrated that as-synthesized SiNPs were an outstanding candidate for fluorescent materials. The UV-Vis spectrum shows absorption peak at 350 nm while the maximum fluorescence emission intensity centered at 450 nm when excited at 350 nm.

Mechanism of the fluorescent detection method

The feasibility of using SiNPs for Cu^{2+} detection was explored. Fig. 2 shows the fluorescence spectra of SiNPs solution under various conditions. It can be seen that under the 350 nm light excitation, the SiNPs exhibits a strong fluorescence emission peak centre at 450 nm. The presence of Cu^{2+} or Cys alone does not affect the fluorescence of SiNPs. However, presence of both Cu^{2+} and Cys leads to an obvious decrease of fluorescence intensity of SiNPs, indicating that Cu^{2+} and Cys can quench the fluorescence of SiNPs effectively. These results indicate that it is feasible to quantify Cu^{2+} by measuring the fluorescence intensity of SiNPs.

The quenching mechanism was investigated. Previously study indicated that the Cu^{2+} can catalyze the oxidation of Cys to cystine and produce H_2O_2 under the O_2 atmosphere [22, 23]. The overall process of Cys oxidation as:



The authors inferred that the Cu^{2+} can further catalyze the decomposition of H_2O_2 to produce hydroxyl radicals through a Fenton-like reaction [24, 25]. Similar to the reported carbon quantum dots [28, 29] and semiconductor quantum dots [30], the authors further inferred that the surface states of SiNPs may be destroyed and changed by the generated hydroxyl radicals, which results the fluorescence quenching of SiNPs. Control experiments were carried out to demonstrate the fluorescence quenching mechanism. As shown in Fig. S1, the H_2O_2 , cystine, cystine+ H_2O_2 cystine+ Cu^{2+} do not affect the fluorescence of SiNPs. Conversely, as shown in Fig. S1B, the fluorescence of SiNPs was quenched effectively in the presence of both Cu^{2+} and H_2O_2 . Furthermore, the fluorescence quenching efficiency was decreased to a certain degree when dimethyl sulfoxide (DMSO, a trapping agent of hydroxyl radicals) was added to the solution (Fig. S2A). These results indirectly indicated that the hydroxyl radicals are associated with the fluorescence quenching of SiNPs. Similar to the published literatures that the high activity hydroxyl radicals can destroy the original surface state of SiNPs, resulting the fluorescence quenching of SiNPs [31]. Fig. S2B shows the fluorescence recovers to a certain degree when NaBH_4 is added to the solution. Therefore, the authors speculated that the fluorescence quenching of SiNPs was caused by the changes of the surface state of SiNPs through hydroxyl radicals. The detection mechanism is shown in Fig. 3.

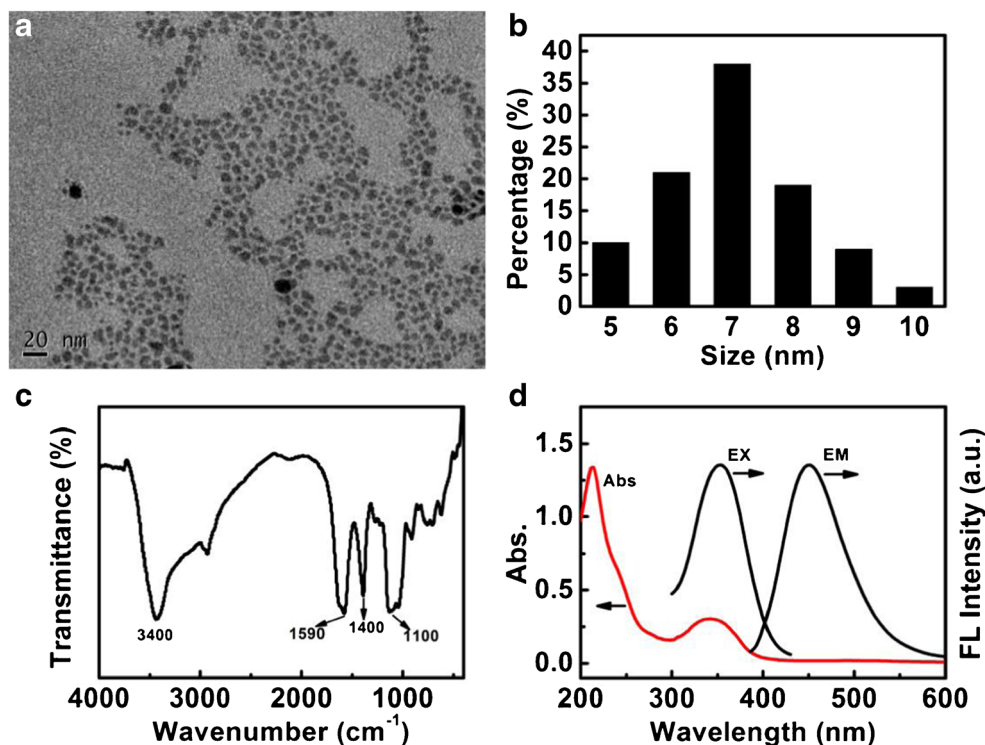
Optimization of method

The following parameters were optimized: (a) the concentration of Cys; (b) the concentration of SiNPs; (c) pH and (d) incubation time. Respective data and figures are given in the Electronic Supporting Material (Fig. S3). The following experimental conditions were found to give the best results: (a) the concentration of Cys is 0.5 mM; (b) pH = 8; (c) the concentration of SiNPs is $12\text{ }\mu\text{g mL}^{-1}$ and (d) an incubation time of 30 min.

The analytical performance of the method

Under optimal conditions, the analytical performance of the method for Cu^{2+} detection was evaluated. Fig. 4a shows the fluorescence emission spectra of the SiNPs in the presence of various concentrations of Cu^{2+} . It can be seen that the fluorescence of SiNPs at 450 nm decreased gradually with the increasing of Cu^{2+} . The relationship between the fluorescence quenching rate of SiNPs $[(F_0-F)/F_0]$ and the concentration of Cu^{2+} is shown in Fig. 4b. It is clearly seen that a good linear correlation is observed over the concentration range of 0.05 μM to 15 μM . The corresponding calibration equation is $y = 0.0424x + 0.0663$ ($R^2 = 0.9984$), where y and x are the fluorescence quenching rate $[(F_0-F)/F_0]$ and the concentration

Fig. 1 **a** TEM image of the SiNPs. **b** Size distribution histograms of SiNPs. **c** FT-IR spectrum of the SiNPs. **(D)** UV-vis absorption spectrum, excitation spectrum and emission spectrum of SiNPs



of Cu^{2+} , respectively. According to the ratio of 3 times the standard deviation of the blanks to the slope of the linear equation of the calibration curve, the limit of detection (LOD) is calculated as 29 nM. The LOD is lower than the maximum concentration of Cu^{2+} in drinking water by the US Environmental Protection Agency (20 μM). Table 1 summarizes some nanomaterials-based fluorescence method for Cu^{2+} analysis [2, 18–21, 32–39]. Some metal ions with similar chemical properties or ionic radius may affect the interaction between Cu^{2+} and the fluorescence nanomaterials. Thus, these detection methods had lower selectivity to Cu^{2+} . J. Hwang et al. reported a fluorescence method for the detection of

Cu^{2+} by using electrochemically etch method synthesized porous silicon nanoparticles as a fluorescent probe [39]. However, the detection mechanism of J. Hwang and his co-worker is different from the present method. The method of J. Hwang and his coworker was based on the interaction between Cu^{2+} and porous silicon nanoparticles, which may be affected by Fe^{2+} . Conversely, the present method has good selectivity toward Cu^{2+} due to the dual catalytic effects of Cu^{2+} . Therefore, the authors believe that they provide an effective new approach for the selective detection of Cu^{2+} .

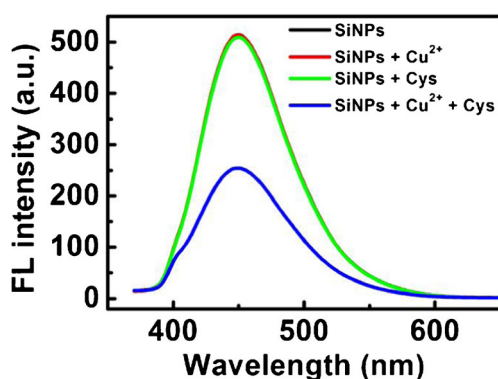


Fig. 2 The fluorescence spectra of SiNPs in the presence of Cu^{2+} , Cys and Cu^{2+} +Cys. Experiments were performed in HEPES buffer (pH 8.0, 10 mM), the concentration of SiNPs, Cu^{2+} and Cys are 12 $\mu\text{g mL}^{-1}$, 10 μM and 0.5 mM, respectively, the excitation/emission wavelengths are 350/450 nm, slits width are both 5 nm)

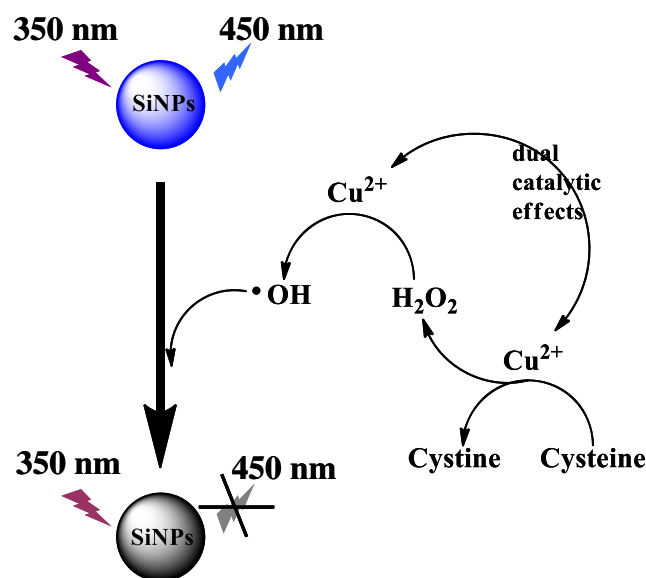
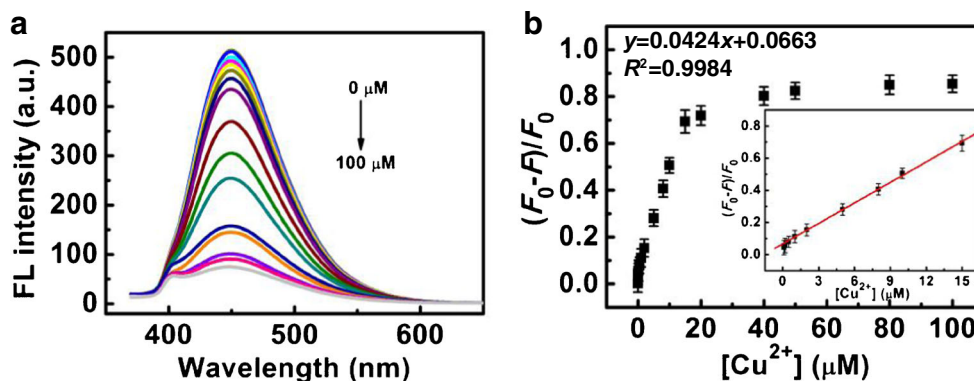


Fig. 3 Schematic illustration for the detection of Cu^{2+}

Fig. 4 **a** Fluorescence spectra of SiNPs+Cys in the presence of different concentrations of Cu^{2+} . **b** The relationship between the fluorescence quenching rate and the concentration of Cu^{2+} ; Inset shows the calibration curve at low concentrations. (Performed in HEPES buffer (pH 8.0, 10 mM), the concentration of SiNPs, and Cys are $12 \mu\text{g mL}^{-1}$ and 0.5 mM , respectively. F_0 and F correspond to the fluorescence intensity of the SiNPs at 450 nm in the absence and presence of Cu^{2+} , respectively. The excitation wavelength is 350 nm , slit width are both 5 nm . The error bars represent standard deviation from 3 replicates, and magnified by a factor of three)



Next, the fluorescence quenching data were further analyzed by the Stern-Volmer equation:

$$I_0/I = K_{SV} \times c_Q + 1$$

Where I_0 and I are the fluorescence intensities of SiNPs in the absence and presence of Cu^{2+} , respectively; c_Q is the concentration of the Cu^{2+} ; K_{SV} is the Stern-Volmer quenching constant. As

shown in Fig. S4, the data do not fit a conventional linear Stern-Volmer equation, indicating both dynamic and static quenching processes occur in the present detection method [19, 36].

In order to evaluate the selectivity of this method for the detection of Cu^{2+} , various relevant metal ions such as Na^+ , K^+ , Ag^+ , Mg^{2+} , Ni^{2+} , Zn^{2+} , Ca^{2+} , Co^{2+} , Cd^{2+} , Hg^{2+} , Pb^{2+} , Mn^{2+} , Fe^{2+} , Fe^{3+} , and Al^{3+} were investigated. As shown in Fig. 5a,

Table 1 Comparisons of analytical performances of various nanomaterials-based methods for Cu^{2+} detection

Nanomaterials	Mechanism	Linear range	limit of detection	Major interfering ions	Reference
carbon nanoparticles	interaction between Cu^{2+} and oxygen groups	0-10 μM	23 nM	Co^{2+} , Fe^{2+} , Hg^{2+} , Mn^{2+} , Ni^{2+} , Fe^{3+}	[2]
carbon nanoparticles	interaction between Cu^{2+} and amino groups	0.01-1.1 μM	6 nM	Ni^{2+} , Fe^{2+} , Hg^{2+}	[18]
polymer nanodots	chelation of Cu^{2+} with N and O atoms	Not mentioned	1 nM	Fe^{3+}	[19]
g- C_3N_4 nanosheets	chelation of Cu^{2+} with N atoms	0-10 μM	0.5 nM	Fe^{3+}	[20]
silver nanoparticles	coordination between Cu^{2+} and N, O atoms	0.05-8 μM	Not mentioned	Fe^{2+} , Fe^{3+} , Pb^{2+} , Hg^{2+} , Cd^{2+}	[21]
europium-decorated graphene quantum dots	interaction between Cu^{2+} and oxygen groups	0.1-10 μM	56 nM	Ni^{2+}	[32]
carbon nanoparticles	interaction between Cu^{2+} and amino groups	0-15 μM	47 nM	Fe^{3+} , Hg^{2+}	[33]
carbon nanoparticles	coordination between Cu^{2+} and N atoms	0.2-1 μM	36 nM	Hg^{2+}	[34]
carbon nanoparticles	chelation and electrostatic attraction between Cu^{2+} and N, O atoms	0.833-833 μM	300 nM	Ni^{2+}	[35]
1-(2-thiazolylazo)-2-naphthol-passivated CdTe NCs	electron or energy transfer between Cu^{2+} and the probe	0.0233-23.3 μM	0.5 nM	Ag^+ , Pb^{2+} , Fe^{3+} , Hg^{2+} , Cr^{3+}	[36]
gold nanoparticles	coordination between Cu^{2+} and $[\text{Au}(\text{OH})_4]^-$	0.2-6 μM	40 nM	Ni^{2+} , Mn^{2+} , Co^{2+}	[37]
silver-coated gold nanorods	catalytic leaching between Cu^{2+} , $\text{S}_2\text{O}_3^{2-}$, and the surface of the Au@Ag nanorods	0.003-1 μM	3 nM	Hg^{2+}	[38]
porous silicon nanoparticles	interaction between Cu^{2+} and porous silicon nanoparticles	0-200 μM	100 nM	Fe^{2+}	[39]
silicon nanoparticles	dual catalytical effects of Cu^{2+}	0.05-15 μM	29 nM	good selectivity	This work

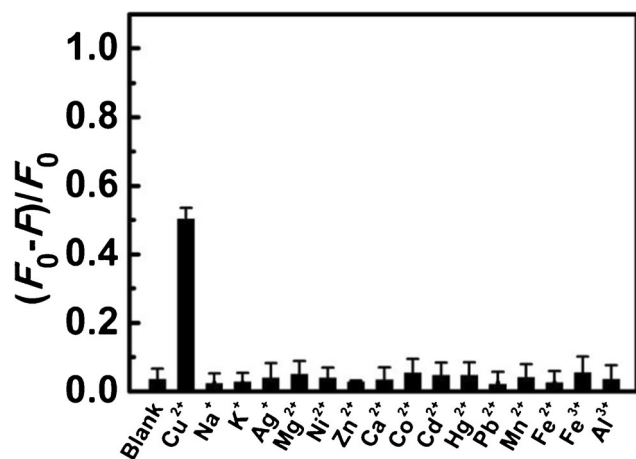


Fig. 5 The fluorescence quenching rate of SiNPs in the presence of Cu²⁺ and other compounds. (Performed in HEPES buffer (pH 8.0, 10 mM), the concentration of SiNPs, and Cys are 12 $\mu\text{g mL}^{-1}$ and 0.5 mM, respectively. The concentration of Cu²⁺ is 10 μM , other compounds is 200 μM . F_0 and F correspond to the fluorescence intensity of the SiNPs at 450 nm in the absence and presence of interfering substance, respectively. The excitation wavelength is 350 nm, slit width are both 5 nm. The error bars represent standard deviation from 3 replicates, and magnified by a factor of three)

the fluorescence quenching rate caused by Cu²⁺ is greater than that of other metal ions, indicating that this method has a good selectivity for Cu²⁺ detection. Although the Fe²⁺ can react with H₂O₂ to generate hydroxyl radicals, the Fe²⁺ can not catalytic the Cys to produce H₂O₂. Thus, the authors speculate that the selectivity may be due to the unique catalytic reaction between Cu²⁺ and Cys [22, 23].

Analysis of Cu²⁺ in real water samples

The practicality of this method to detection of Cu²⁺ in real samples was further validated by a standard addition method. Certain concentration of Cu²⁺ standard solutions were directly spiked into the real water samples (tap water, mineral water, river water) before sample pre-treatment. The analysis results are summarized and listed in Table S1. Satisfactory recoveries (94.0%–105.8%) were obtained for all samples, implying that this method has potential application in the detection of Cu²⁺ in real applications.

Conclusions

In summary, a novel and effective fluorometric method for the detection of Cu²⁺ has been developed. It is based on the excellent fluorescence properties of SiNPs as well as the the dual catalytical effects of Cu²⁺. Under the optimal conditions, a relative low detection limit and a good linear for Cu²⁺ were obtained. Compared with other reported Cu²⁺ methods which commonly based on the interaction between Cu²⁺ and the surface groups of the nanomaterials, this method has better

selectivity due to the dual catalytical effects of Cu²⁺. In addition, this method can be applied to the detection of Cu²⁺ in real samples and obtained satisfactory results, indicating its potential application in practice. This research will provide an effective new approach for the design of Cu²⁺ selective detection method. Nonetheless, it should be noted that this novel method also has a limitation. As the rapid and on-site detection of Cu²⁺ is of great significance to human health and pollution treatment. The detection time of this method is 30 min and the response is irreversible, which limits its online detection application. However, this method is still expected for sensitive and reliable detection of Cu²⁺ due to its high selectivity.

Acknowledgments This work was supported by the National Natural Science Foundation of China (21475043, 21675051 and 21375037).

Compliance with ethical standards

The authors declare that they have no competing interests.

References

1. Brown DR, Kozlowski H (2004) Biological inorganic and bioinorganic chemistry of neurodegeneration based on prion and Alzheimer diseases. *Dalton Trans* 13:1907–1917
2. Zong J, Yang X, Trinchi A, Hardin S, Cole I, Zhu Y, Li C, Muster T, Wei G (2014) Carbon dots as fluorescent probes for “off-on” detection of Cu²⁺ and L-cysteine in aqueous solution. *Biosens Bioelectron* 51:330–335
3. Brady DC, Crowe MS, Turski ML, Hobbs GA, Yao X, Chaikwad A, Knapp S, Xiao K, Campbell SL, Thiele DJ, Counter CM (2014) Copper is required for oncogenic BRAF signalling and tumorigenesis. *Nature* 509(7501):492–496
4. Salinas-Castillo A, Ariza-Avidad M, Pritz C, Camprubi-Robles M, Fernandez B, Ruedas-Rama MJ, Megia-Fernandez A, Lapresta-Fernandez A, Santoyo-Gonzalez F, Schrott-Fischer A, Capitan-Vallvey LF (2013) Carbon dots for copper detection with down and upconversion fluorescent properties as excitation sources. *Chem Commun* 49(11):1103–1105
5. Smith SR, Zhou C, Baron JY, Choi Y, Lipkowski J (2016) Elucidating the interfacial interactions of copper and ammonia with the sulfur passive layer during thiosulfate mediated gold leaching. *Electrochim Acta* 210:925–934
6. Wu J, Boyle EA (1997) Low blank preconcentration technique for the determination of lead, copper, and cadmium in small-volume seawater samples by isotope dilution ICPMS. *Anal Chem* 69(13):2464–2470
7. Cassella RJ, Magalhães OIB, Couto MT, Lima ELS, Neves MAFS, Coutinho FMB (2005) Synthesis and application of a functionalized resin for flow injection/F AAS copper determination in waters. *Talanta* 67(1):121–128
8. Xu X, Daniel WL, Wei W, Mirkin CA (2010) Colorimetric Cu²⁺ detection using DNA-modified gold-nanoparticle aggregates as probes and click chemistry. *Small* 6(5):623–626
9. Song HD, Choi I, Lee S, Yang YI, Kang T, Yi J (2013) On-chip colorimetric detection of Cu²⁺ ions via density-controlled plasmonic core–satellites nanoassembly. *Anal Chem* 85(16):7980–7986

10. Liu L, Dan F, Liu W, Lu X, Han Y, Xiao S, Lan H (2017) A high-contrast colorimetric and fluorescent probe for Cu^{2+} based on benzimidazole-quinoline. *Sensors Actuators B Chem* 247:445–450
11. Tang S, Wang M, Li Z, Tong P, Chen Q, Li G, Chen J, Zhang L (2017) A novel sensitive colorimetric sensor for Cu^{2+} based on in situ formation of fluorescent quantum dots with photocatalytic activity. *Biosens Bioelectron* 89:866–870
12. Su Y-T, Lan G-Y, Chen W-Y, Chang H-T (2010) Detection of copper ions through recovery of the fluorescence of DNA-templated copper/silver nanoclusters in the presence of mercaptopropionic acid. *Anal Chem* 82(20):8566–8572
13. Xu G, Wang J, Si G, Wang M, Xue X, Wu B, Zhou S (2016) A novel highly selective chemosensor based on curcumin for detection of Cu^{2+} and its application for bioimaging. *Sensors Actuators B Chem* 230:684–689
14. Huang C-B, Li H-R, Luo Y, Xu L (2014) A naphthalimide-based bifunctional fluorescent probe for the differential detection of Hg^{2+} and Cu^{2+} in aqueous solution. *Dalton Trans* 43(21):8102–8108
15. Guo Y, Zhang L, Zhang S, Yang Y, Chen X, Zhang M (2015) Fluorescent carbon nanoparticles for the fluorescent detection of metal ions. *Biosens Bioelectron* 63:61–71
16. You Q-H, Lee AW-M, Chan W-H, Zhu X-M, Leung KC-F (2014) A coumarin-based fluorescent probe for recognition of Cu^{2+} and fast detection of histidine in hard-to-transfect cells by a sensing ensemble approach. *Chem Commun* 50(47):6207–6210
17. Kim MH, Jang HH, Yi S, Chang S-K, Han MS (2009) Coumarin-derivative-based off-on catalytic chemodosimeter for Cu^{2+} ions. *Chem Commun* 32:4838–4840
18. Dong Y, Wang R, Li G, Chen C, Chi Y, Chen G (2012) Polyamine-functionalized carbon quantum dots as fluorescent probes for selective and sensitive detection of copper ions. *Anal Chem* 84(14):6220–6224
19. Liu S, Tian J, Wang L, Zhang Y, Qin X, Luo Y, Asiri AM, Al-Youbi AO, Sun X (2012) Hydrothermal treatment of grass: a low-cost, green route to nitrogen-doped, carbon-rich, photoluminescent polymer nanodots as an effective fluorescent sensing platform for label-free detection of $\text{Cu}(\text{II})$ ions. *Adv Mater* 24(15):2037–2041
20. Tian J, Liu Q, Asiri AM, Al-Youbi AO, Sun X (2013) Ultrathin graphitic carbon nitride nanosheet: a highly efficient fluorosensor for rapid, ultrasensitive detection of Cu^{2+} . *Anal Chem* 85(11):5595–5599
21. Ma Y-r, Niu H-y, Zhang X-l, Cai Y-q (2011) Colorimetric detection of copper ions in tap water during the synthesis of silver/dopamine nanoparticles. *Chem Commun* 47(47):12643–12645
22. Buzuk M, Brinić S, Vladislavić N, Bralić M, Buljac M, Rončević IŠ (2016) Real-time monitoring of “self-oxidation” of cysteine in presence of Cu^{2+} : novel findings in the oxidation mechanism. *Monatsh Chem* 147(2):359–367
23. Pecci L, Montefoschi G, Musci G, Cavallini D (1997) Novel findings on the copper catalysed oxidation of cysteine. *Amino Acids* 13(3):355–367
24. Masarwa M, Cohen H, Meyerstein D, Hickman DL, Bakac A, Espenson JH (1988) Reactions of low-valent transition-metal complexes with hydrogen peroxide. Are they “Fenton-like” or not? 1. The case of Cu^+aq and Cr^{2+}aq . *J Am Chem Soc* 110(13):4293–4297
25. Ozawa T, Hanaki A (1991) The first ESR spin-trapping evidence for the formation of hydroxyl radical from the reaction of copper(II) complex with hydrogen peroxide in aqueous solution. *J Chem Soc Chem Commun* 5:330–332
26. Feng Y, Liu Y, Su C, Ji X, He Z (2014) New fluorescent pH sensor based on label-free silicon nanodots. *Sensors Actuators B Chem* 203:795–801
27. Zhong Y, Peng F, Bao F, Wang S, Ji X, Yang L, Su Y, Lee S-T, He Y (2013) Large-scale aqueous synthesis of fluorescent and biocompatible silicon nanoparticles and their use as highly photostable biological probes. *J Am Chem Soc* 135(22):8350–8356
28. Wang H, Lu Q, Hou Y, Liu Y, Zhang Y (2016) High fluorescence, S, N co-doped carbon dots as an ultra-sensitive fluorescent probe for the determination of uric acid. *Talanta* 155:62–69
29. Wei J, Ren J, Liu J, Meng X, Ren X, Chen Z, Tang F (2014) An eco-friendly, simple, and sensitive fluorescence biosensor for the detection of choline and acetylcholine based on C-dots and the Fenton reaction. *Biosens Bioelectron* 52:304–309
30. Mancini MC, Kairdolf BA, Smith AM, Nie S (2008) Oxidative quenching and degradation of polymer-encapsulated quantum dots: new insights into the long-term fate and toxicity of nanocrystals in vivo. *J Am Chem Soc* 130(33):10836–10837
31. Chen Q, Liu M, Zhao J, Peng X, Chen X, Mi N, Yin B, Li H, Zhang Y, Yao S (2014) Water-dispersible silicon dots as a peroxidase mimetic for the highly-sensitive colorimetric detection of glucose. *Chem Commun* 50(51):6771–6774
32. Lin L, Song X, Chen Y, Rong M, Wang Y, Zhao L, Zhao T, Chen X (2015) Europium-decorated graphene quantum dots as a fluorescent probe for label-free, rapid and sensitive detection of Cu^{2+} and L-cysteine. *Anal Chim Acta* 891:261–268
33. Das P, Ganguly S, Bose M, Mondal S, Das AK, Banerjee S, Das NC (2017) A simplistic approach to green future with eco-friendly luminescent carbon dots and their application to fluorescent nanosensor “turn-off” probe for selective sensing of copper ions. *Mater Sci Eng C* 75:1456–1464
34. Lu L, Feng C, Xu J, Wang F, Yu H, Xu Z, Zhang W (2017) Hydrophobic-carbon-dot-based dual-emission micelle for ratiometric fluorescence biosensing and imaging of Cu^{2+} in liver cells. *Biosens Bioelectron* 92:101–108
35. Lin Y, Wang C, Li L, Wang H, Liu K, Wang K, Li B (2015) Tunable fluorescent silica-coated carbon dots: a synergistic effect for enhancing the fluorescence sensing of extracellular Cu^{2+} in rat brain. *ACS Appl Mater Interfaces* 7(49):27262–27270
36. Chao M-R, Hu C-W, Chen J-L (2016) Fluorometric determination of copper(II) using CdTe quantum dots coated with 1-(2-thiazolylazo)-2-naphthol and an ionic liquid. *Microchim Acta* 183(4):1323–1332
37. Deng H-H, Li G-W, Liu A-L, Chen W, Lin X-H, Xia X-H (2014) Thermally treated bare gold nanoparticles for colorimetric sensing of copper ions. *Microchim Acta* 181(9):911–916
38. Wang X, Chen L, Chen L (2014) Colorimetric determination of copper ions based on the catalytic leaching of silver from the shell of silver-coated gold nanorods. *Microchim Acta* 181(1):105–110
39. Hwang J, Hwang MP, Choi M, Seo Y, Jo Y, Son J, Hong J, Choi J (2016) Sensitive detection of copper ions *via* ion-responsive fluorescence quenching of engineered porous silicon nanoparticles. *Sci Rep* 6:35565–35565